Magnetic and ferroelectric orders in strained $Gd_{1/2}Na_{1/2}TiO_3$: First-principles calculations

P. X. Zhou,[1,3] S. Dong,[2,a)] Y. L. Xie,[1] Z. B. Yan,[1] X. H. Zhou,[1] and J.-M. Liu[1,b)]
[1]*Laboratory of Solid State Microstructures and Innovation Center of Advanced Microstructures, Nanjing University, Nanjing 210093, China*
[2]*Department of Physics, Southeast University, Nanjing 211189, China*
[3]*School of Science, Nantong University, Nantong 226007, China*

(Presented 4 November 2014; received 21 September 2014; accepted 3 December 2014; published online 8 April 2015)

The emergent magnetic and ferroelectric orders in A-site ordered $Gd_{1/2}Na_{1/2}TiO_3$ under lattice strain are investigated using the first-principles calculations. It is revealed that the lattice prefers the perovskite structure with alternatively stacked Ga-O and Na-O layers along the *b*-axis and the ground spin state favors the G-type antiferromagnetic (G-AFM) order. The *ac*-plane biaxial strain can remarkably tune the amplitude of ferroelectric polarization, while the G-AFM spin structure is robustly unaffected. The ±4% strains can trigger the change of polarization up to ±50% relative to the polarization value of unstrained structure. The present work suggests a possible scenario to control emergent multiferroic behaviors in $Gd_{1/2}Na_{1/2}TiO_3$ via lattice strain. © *2015 AIP Publishing LLC*.
[http://dx.doi.org/10.1063/1.4917060]

Sodium doped rare-earth titanates $Ln_{1/2}Na_{1/2}TiO_3$ (Ln = La ~ Yb except Ce and Pm) (LnNTO) have been evidenced for their quantum paraelectricity in experiments.[1] Quantum paraelectrics represent a class of materials with attractive dielectric and thermodynamic behaviors, such as temperature (T) independent dielectric constant below certain temperature T_a.[2,3] It is known that the dielectric constant (ε) below temperature T_s ($T_s > T_a$) complies the Barrett's law instead of the Curie-Weiss law, leading to the low-T dielectric plateau. Comparing with the typical quantum paraelectric $SrTiO_3$ (STO) whose T_s and T_a are ~35 K and ~4 K, respectively, LnNTO compounds usually have much higher T_s and T_a. Moreover, all LnNTO compounds have the *Pnma* structure.[4,5] The dielectric response is substantially dependent on the Ln ionic size and thus the lattice distortion, including the rotation and tilting of Ti octahedra. It was revealed that the dielectric plateau at $T \to 0$ falls and the values of both T_a and T_s increase with the atomic number from La to Yb or with the distortion magnitude of Ti-octahedra. In addition, the energy band-gap increases with the distortion of Ti-octahedra.[6] All these features suggest significant difference of the underlying physics of LnNTO from that revealed in STO, which does not have the distortion of Ti octahedra.[7]

In quantum paraelectrics, although the ferroelectricity is suppressed by the zero point motion, the ferroelectricity can be stimulated by the strain as in the strained STO, $KTaO_3$, and $CaTiO_3$ films.[8–11] This characteristic promises high sensitivity of the dielectric and ferroelectric properties to internal or external stimuli.

So far, the structural distortion and dielectric/optical responses of LnNTO compounds have been preliminarily investigated and the role of the 4*f* electrons has been rarely addressed.[4,6,12–16] Here, two prominent issues should be mentioned. First, the Ln species mostly show big 4*f* moments. The Ln^{3+} and Na^{1+} valence charges may drive the charge fluctuations of Ti species. Second, lattice strain has been demonstrated to be powerful in tuning the emergent ferroelectricity of oxides.[11,17–19] Especially for quantum paraelectrics, the lattice strain is highly possible to enhance the ferroelectric soft mode over the zero point vibration energy, leading to the ferroelectricity. Nevertheless, quite rare work touching the structure and magnetism of LnNTO in response to lattice distortion and strain is available.

In this work, we choose one member of this family, $Gd_{1/2}Na_{1/2}TiO_3$ (GNTO), as the object of the present first-principles calculations. We address the chemical configuration, electronic structure, and magnetism of GNTO, noting that Gd^{3+} has the biggest 4*f* moments. In particular, we will focus on the possible ferroelectric generation/modulation and magnetic ground states in response to tensile and compressive strain. It is also of significance to search for the mechanism of strain driven ferroelectricity variation in such magnetic materials.

The first-principles calculations are performed using the Vienna *ab-initio* Simulation Package (VASP).[20,21] The exchange correction potential used here is the generalized gradient approximation (GGA). It is believed that there exists strong Coulomb interactions for the *d*- and *f*-electrons, and therefore the Hubbard U is imposed on the Gd's *f*-orbitals. The Liechtenstein method[22] is employed with $U = 6.7$ eV and Hund exchange $J = 0.7$ eV, as done in previous studies.[23–25] The plane-wave energy cutoff is 500 eV and the Hellman-Feynman forces are all below 0.01 eV/Å during the optimization. The Monkhorst-Pack *k*-point mesh is $7 \times 5 \times 7$ for bulks and $7 \times 3 \times 7$ for the structures with spin degree of freedom (the supercell is $1 \times 2 \times 1$ unit cells), respectively.

First, for GNTO, the chemically ordered or disordered occupations of Gd and Na species at the A-site should be discussed. In spite of the possible Gd/Na disorder occupation, for practical computations, the chemical order structure is usually

a)Electronic mail: sdong@seu.edu.cn.
b)Electronic mail: liujm@nju.edu.cn.

adopted.[5] It should be mentioned that the claimed chemical configuration as inferred from experiments on polycrystalline samples is the disordered Gd/Na occupation, while the ground state for chemical occupation remains an open issue. Here, we only investigate the chemical ordered cases of GNTO. Following the experimental orthorhombic structure, we choose one unit cell consisting of 20 atoms for the following calculations. Considering the positions of two Na (or Gd) atoms and lattice symmetry, the unit cell has three kinds of crystal structures, as schematically shown in Fig. 1. In the crystal structure 1, A-site cations Na and Gd occupy different layers along the [010] axis, while in the crystal structure 2, Na and Gd occupy the different layers along the [100] axis. In the crystal structure 3, Na and Gd ions are alternatively arranged along both the [010] and [100] axes. Full-scale optimizations of the three kinds of crystal structures have been performed, keeping the orthorhombic framework without counting the Gd^{3+} magnetism. It is shown that the crystal structure 1 has the lowest total energies, which are 0.624 eV and 0.460 eV lower than that of crystal structures 2 and 3, respectively. The optimized lattice constants for structure 1 are $a_0 = 5.512$ Å, $b_0 = 7.738$ Å, and $c_0 = 5.387$ Å, respectively. The structure 1, which consists of stacking Na-O and Gd-O layers, can be considered as an $1+1$ superlattice grown along the [010] axis. In this sense, such a superlattice structure can be tuned by substrate strains.

Second, we add the spin degree of freedom of Gd atoms and perform again the full-scale optimization of the three structures in bulk form so that the magnetic ground state can be obtained. For such calculations, the lattice dimension is expanded along the *b*-axis and two unit cells (40 atoms) with pre-imposed spin configurations are chosen. The spin orders under consideration include A-type antiferromagnetic (A-AFM), C-type AFM (C-AFM), G-type AFM (G-AFM), and ferromagnetic (FM) orders. The result shows that the crystal structure 1 is still the ground state and the lattice constants are almost unchanged after considering the magnetism. The calculated total energies for the A-AFM, C-AFM, and FM orders of crystal structure 1 are 2.2 meV, 0.015 meV, and 2.2 meV, taking the energy of the G-AFM order as the reference state. This energy difference is very weak, implying a low Néel temperature. Here, it should be mentioned that the C-AFM order has nearly the same energy as the G-AFM one, namely, the energy difference is beyond the precision of our density functional theory (DFT) calculations. Similar energy degeneration is also observed between the A-AFM and FM states. One is allowed to argue that the (010) in-plane spin structure favors the AFM order, while the out-plane spin coupling should be very weak due to the long distance between the nearest-neighbor Gd-O layers (separated by Na-O layers). Therefore, both the FM coupling and AFM coupling along the *b*-axis may be possible if any.

Third, the biaxial strains are imposed on the lattice along both the *a*-axis and *c*-axis, leaving the lattice constant along the *b*-axis and the inner atomic positions to be fully relaxed. The lattice strain is defined as $\delta = (a - a_0)/a_0 = (c - c_0)/c_0$, here, a (c) and a_0 (c_0) are the lattice constants of the strained and unstrained lattices, respectively. In the present work, we only consider the cases of biaxial strain, i.e., the strains along the *a*-axis and *c*-axis are identical, and only consider the crystal structure 1 under all the consideration strain. The optimized lattice constants under strains are showed in Fig. 2(a). As expected, the *b*-axis lattice constant increases with the decreasing lattice constants along the *a*- and *c*-axes. When taking into account the ordering of Na and Gd, the space groups for both the unstrained and strained lattices

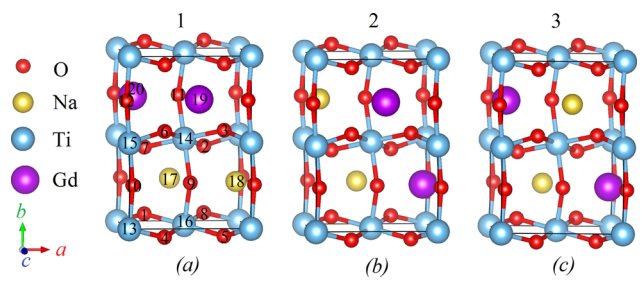

FIG. 1. Schematic crystal structures of the three possible chemical configurations of GNTO. Here, each ion of crystal structure 1 (a) is indexed numerically.

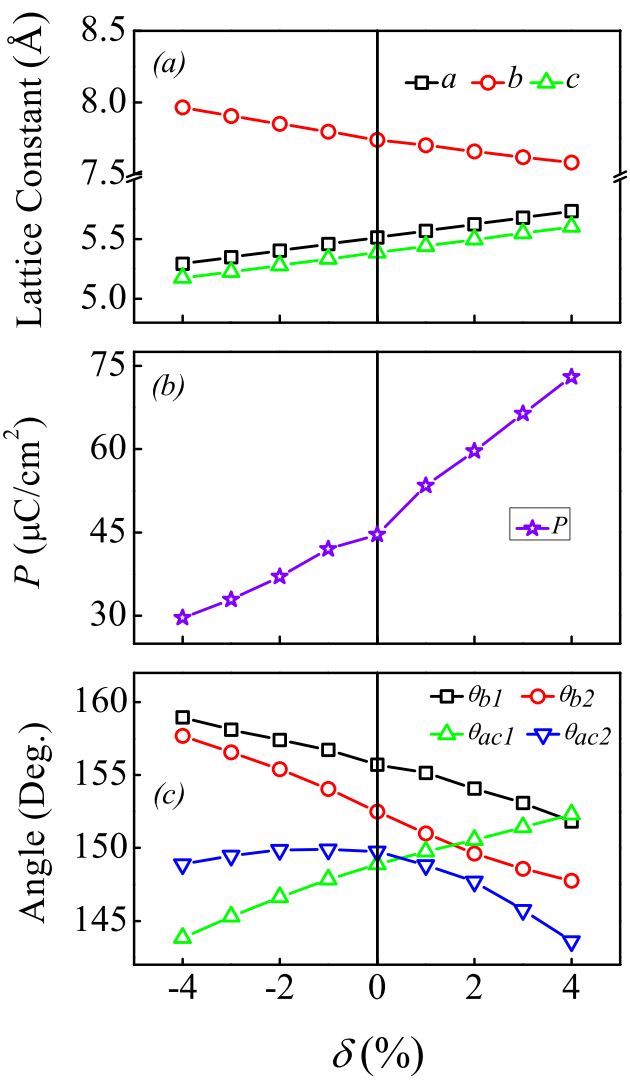

FIG. 2. (a) The *a*, *b*, and *c* lattice constants as a function of strain δ. (b) Evaluated magnitude of spontaneous polarization *P* as a function of strain δ, which is along the *a*-axis. (c) The strain dependence of out-plane angles θ_{b1}, θ_{b2} and in-plane angles θ_{ac1}, θ_{ac2}.

become $Pmc2_1$, whose point group is *mm2*. Such a *mm2* point group belongs to the polar point group family, which lacks the space inversion symmetry and thus allows the ferroelectricity. Therefore, the ferroelectricity is naturally expected even for the unstrained structure of the chemical ordered GNTO.

Although experimentally the A-site disordered LnNTO is quantum paraelectric, previous theoretical investigations found evidences for ferroelectric soft mode existing in A-site ordered LnNTO.[5] In fact, the A-site ordered GNTO studied here, can be considered as a $1+1$ superlattice structure growing along the [010] axis as mentioned above. Due to the different rotation angles between two materials, such type of $(ABO_3)_n$–$(A'BO_3)_n$ superlattices will be ferroelectric when n is an odd number.[26,27]

To explore the ferroelectricity in the strained and unstrained lattices, the standard Berry-phase method is employed to evaluate the ferroelectric polarization (P). As plotted in Fig. 2(b), both the tensile and compressive strains can tune the magnitude of spontaneous polarization up to ~50% (under ±4% strains). Particularly, the polarization is enhanced by increasing tensile strain, but is suppressed under the compressive strain. All polarizations shown in Fig. 2 are along the *a*-axis, while the polarizations along the *b*- and *c*-axes are both zero.

According to Benedek and Fennie's proposal,[28] we evaluate the octahedral distortion which would have some correlation with the polarization. A straightforward characterization is to count the in-plane (*ac*-plane) Ti-O-Ti angle (θ_{ac}) and out-of-plane Ti-O-Ti angle (θ_b), as a function of δ. As shown in Fig. 2(c), since the Na and Gd ion radii are different, there are two different out-of-plane angles and so do the in-plane angles, which are in consistent with the emergent ferroelectricity.[27] In other words, for non-polar structure, there should be only one value for the out-of-plane angles and one value for the in-plane one. The two out-of-plane angles θ_{b1} and θ_{b2} decrease gradually with the increasing δ, as a result of decreasing lattice constant along the *b*-axis. One in-plane angle θ_{ac1} increases monotonously with δ from the compressive side to tensile side, as expected. Another in-plane angle θ_{ac2} is non-monotonous: slightly increases first and then quickly decreases with increasing δ. This behavior is due to the competition between elongated in-plane lattice constants and ferroelectric polarization.

In addition to the distortion angles, we also evaluate the displacement of each atom to illuminate the polarization modulation under strains. First, all atoms in one unit cell are indexed as in Fig. 1(a). Then each atom's displacement of strained lattice from that of the unstrained lattice is characterized by three coordinates (Δx, Δy, Δz) along the *a*-, *b*-, and *c*-axes, respectively, in the fractional coordinate unit (Fcu). Here, we choose the two largest strain cases $\delta = 4\%$ and -4% for illustration, and the results are plotted in Figs. 3(a) and 3(b) where the atom index m from 1 to 12 denotes the oxygen ions, m from 13 to 16 for the Ti ions, m from 17 to 18 for the Na ions, and m from 19 to 20 for the Gd ions, respectively. It is found that the two atoms in each adjacent ion-pair have the opposite Δy and Δz values, i.e., $\Delta y(m = 2n+1) = -\Delta y(m = 2n+2)$ and $\Delta z(m = 2n+1) = -\Delta z(m = 2n+2)$ at $n = 0, 1, 2, \ldots$. Here, this so-called ion-pair is defined from the number index in Fig. 1(a) and it does not mean the spatial atomic pair. This property also applies to other cases of

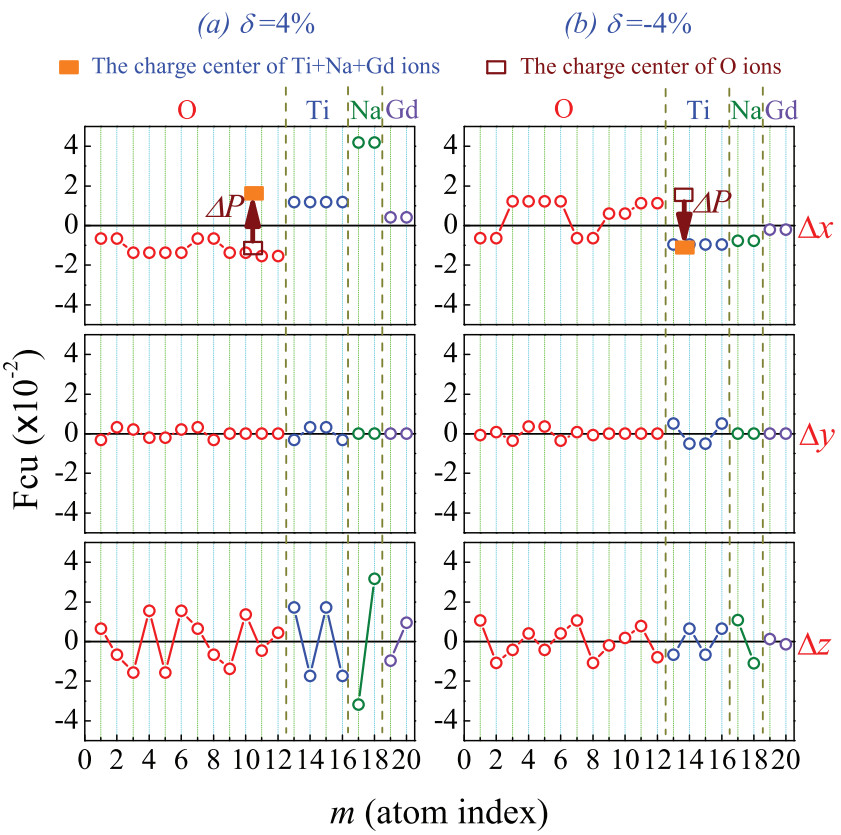

FIG. 3. The displacements of spatial coordinates (Δx, Δy, Δz) of all ions (as indexed in Fig. 1) in the strained crystal structure 1, relative to the corresponding coordinates of these ions in the unstrained lattice: (a) $\delta = 4\%$ and (b) $\delta = -4\%$. The varied spontaneous polarization ΔP along the *a*-axis in each case is labeled by arrows. The displacements are in the fractional coordinate unit (Fcu).

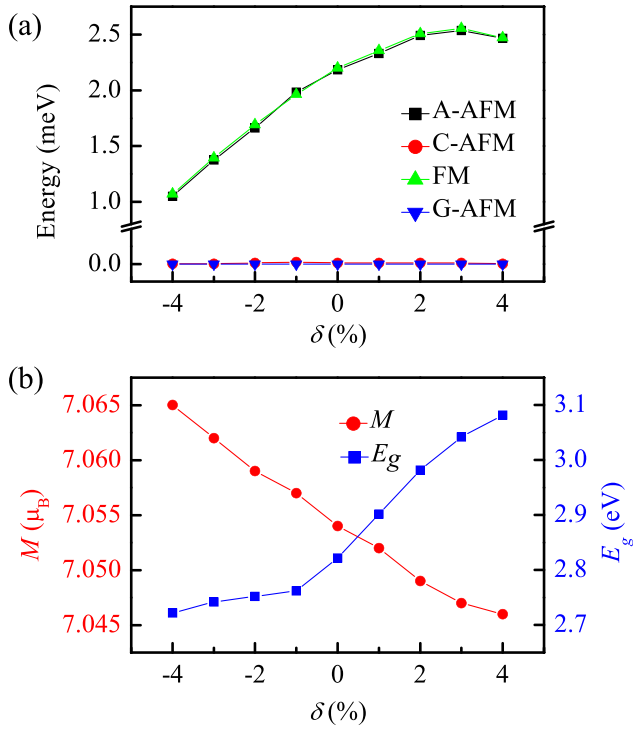

FIG. 4. (a) The strain dependent energies of A-AFM, C-AFM G-ATM, and FM. Here, the G-AFM is taken as the energy reference in all strained/unstrained cases. (b) Evaluated magnetic moment per Gd ion (M) and band-gap (E_g) as a function of strain, respectively.

strain. Such a behavior cancels the net polarizations along the b-axis and c-axis. However, it is very different for Δx. Along the a-axis, the displacement of the charge center of oxygen anions is always in opposite to that of the charge center of all cations, leading to the varied electric dipole, as indicated by the arrows (ΔP). This ΔP, negative for $\delta = -4\%$ and positive for $\delta = 4\%$, together with the original polarization of unstrained lattice, gives rise to the strain-tuned behavior as shown in Fig. 2(b).

Finally, the influence of lattice strain on the magnetic behaviors is investigated. Again, here we take the G-AFM order as the reference state under each strain. The evaluated total energy data are shown in Fig. 4(a). It is found that the G-AFM state remains to be the ground state for both the tensile-strained and compressive-strained lattices. This suggests that the in-plane AFM order is stable against the external strain. In particular, the in-plane tensile strain can strength the G-AFM order comparing with the FM one. Meanwhile, the in-plane lattice expansion slightly suppresses the Gd^{3+} moment, as shown in Fig. 4(b). It is also reasonable that the energy band-gap is widened by the in-plane lattice expansion for larger distortion ((Fig. 2(c)), as shown in Fig. 4(b) too.

In conclusion, the effects of the ac-plane lattice strain on the electronic and magnetic properties of A-site cation ordered $Gd_{1/2}Na_{1/2}TiO_3$ have been investigated using the first-principles calculations. It is revealed that the magnetic ground state is the G-type AFM state which remains unchanged under both the tensile and compressive in-plane strains up to $\pm 4\%$. The tensile and compressive strains, however, can generate remarkable changes of ferroelectric polarizations along the a-axis. The ferroelectricity is relevant with the coherent distortion of the Ti-octahedra. The present work may be informative for strain engineering the emergent ferroelectricity in layered chemical ordered structure of $Ln_{1/2}Na_{1/2}TiO_3$ materials.

This work was supported by the National 973 Projects of China (Grants No. 2011CB922101), the Natural Science Foundation of China (Grants Nos. 11234005, 11374147, 51332006, 51301084), and the Priority Academic Program Development of Jiangsu Higher Education Institutions, China.

[1]P.-H. Sun, T. Nakamura, Y. J. Shan, Y. Inaguma, and M. Itoh, Ferroelectrics **200**, 93 (1997).
[2]K. A. Müller and H. Burkard, Phys. Rev. B **19**, 3593 (1979).
[3]T. Miyamoto, K. Kimura, T. Hamamoto, H. Uemura, H. Yada, H. Matsuzaki, S. Horiuchi, and H. Okamoto, Phys. Rev. Lett. **111**, 187801 (2013).
[4]Y. J. Shan, T. Nakamura, P.-H. Sun, Y. Inaguma, and M. Itoh, Ferroelectrics **218**, 161 (1998).
[5]G. Geneste, J.-M. Kiat, C. Malibert, and J. Chaigneau, Phys. Rev. B **75**, 174107 (2007).
[6]Y. Inaguma, T. Tsuchiya, and T. Katsumata, J. Solid State Chem. **180**, 1678 (2007).
[7]S. E. Rowley, L. J. Spalek, R. P. Smith, M. P. M. Dean, M. Itoh, J. F. Scott, G. G. Lonzarich, and S. S. Saxena, Nat. Phys. **10**, 367 (2014).
[8]S. Glinšek, D. Nuzhnyy, J. Petzelt, B. Malič, S. Kamba, V. Bovtun, M. Kempa, V. Skoromets, P. Kužel, I. Gregora, and M. Kosec, J. Appl. Phys. **111**, 104101 (2012).
[9]C. Filipič, V. Bobnar, Z. Kutnjak, S. Glinšek, B. Kužnik, B. Malič, M. Kosec, and A. Levstik, Europhys. Lett. **96**, 37003 (2011).
[10]H. Moriwake, A. Kuwabara, C. A. J. Fisher, H. Taniguchi, M. Itoh, and I. Tanaka, Phys. Rev. B **84**, 104114 (2011).
[11]A. Antons, J. B. Neaton, K. M. Rabe, and D. Vanderbilt, Phys. Rev. B **71**, 024102 (2005).
[12]R. Garg, A. Senyshyn, H. Boysen, and R. Ranjan, J. Phys.: Condens. Matter **20**, 505215 (2008).
[13]R. M. V. Rao, H. Munekata, K. Shimada, M. Lippmaa, M. Kawasaki, Y. Inaguma, M. Itoh, and H. Koinuma, J. Appl. Phys. **88**, 3756 (2000).
[14]C. Ang, A. S. Bhalla, and L. E. Cross, Phys. Rev. B **64**, 184104 (2001).
[15]G. Geneste, J.-M. Kiat, and C. Malibert, Phys. Rev. B **77**, 052106 (2008).
[16]F. Borodavka, E. Simon, I. Gregora, S. Kamba, R. Haumont, and J. Hlinka, J. Phys.: Condens. Matter **25**, 085901 (2013).
[17]J. H. Lee and K. M. Rabe, Phys. Rev. Lett. **104**, 207204 (2010).
[18]S. Bhattacharjee, E. Bousquet, and P. Ghosez, Phys. Rev. Lett. **102**, 117602 (2009).
[19]J. M. Rondinelli, A. S. Eidelson, and N. A. Spaldin, Phys. Rev. B **79**, 205119 (2009).
[20]G. Kresse and J. Hafner, Phys. Rev. B **47**, 558 (1993).
[21]G. Kresse and J. Furthmüller, Phys. Rev. B **54**, 11169 (1996).
[22]A. I. Liechtenstein, V. I. Anisimov, and J. Zaane, Phys. Rev. B **52**, R5467 (1995).
[23]A. B. Shick, A. I. Liechtenstein, and W. E. Pickett, Phys. Rev. B **60**, 10763 (1999).
[24]C.-G. Duan, R. F. Sabiryanov, J. Liu, W. N. Mei, P. A. Dowben, and J. R. Hardy, Phys. Rev. Lett. **94**, 237201 (2005).
[25]P. Kurz, G. Bihlmayer, and S. Blügel, J. Phys.: Condens. Matter **14**, 6353 (2002).
[26]E. Bousquet, M. Dawber, N. Stucki, C. Lichtensteiger, P. Hermet, S. Gariglio, J.-M. Triscone, and P. Ghosez, Nature (London) **452**, 732 (2008).
[27]J. Alaria, P. Borisov, M. S. Dyer, T. D. Manning, S. Lepadatu, M. G. Cain, E. D. Mishina, N. E. Sherstyuk, N. A. Ilyin, J. Hadermann, D. Lederman, J. B. Claridge, and M. J. Rosseinsky, Chem. Sci. **5**, 1599 (2014).
[28]N. A. Benedek and C. J. Fennie, Phys. Rev. Lett. **106**, 107204 (2011).